

# E(5), X(5), and prolate to oblate shape phase transitions in relativistic Hartree Bogoliubov theory

R. Fossion<sup>a,b1</sup>, Dennis Bonatsos<sup>c2</sup>, and G. A. Lalazissis<sup>a3</sup>

<sup>a</sup> Physics Department, Aristotle University of Thessaloniki  
GR-54124 Thessaloniki, Greece

<sup>b</sup> Istituto Nazionale di Fisica Nucleare and Dipartimento di Fisica Galileo Galilei  
Via Marzolo 8, I-35131 Padova, Italy

<sup>c</sup> Institute of Nuclear Physics, National Center for Scientific Research “Demokritos”  
GR-15310 Aghia Paraskevi, Attiki, Greece

## Abstract

Relativistic mean field theory with the NL3 force is used for producing potential energy surfaces (PES) for series of isotopes suggested as exhibiting critical point symmetries. Relatively flat PES are obtained for nuclei showing the E(5) symmetry, while in nuclei corresponding to the X(5) case, PES with a bump are obtained. The PES corresponding to the Pt chain of isotopes suggest a transition from prolate to oblate shapes at  $^{186}\text{Pt}$ .

## 1 Introduction

Critical point symmetries [1, 2] corresponding to shape phase transitions in nuclear structure are recently receiving considerable attention, since they lead to parameter independent (up to overall scale factors) predictions for spectra and  $B(E2)$  transition rates which compare well with experimental data [3, 4, 5, 6]. The E(5) [1] and X(5) [2] critical point symmetries correspond to special solutions of the Bohr Hamiltonian [7], in both of which an infinite square well potential in the quadrupole ( $\beta$ ) degree of freedom is assumed. In E(5), corresponding to the transition from vibrational [U(5)] to  $\gamma$ -unstable [O(6)] nuclei, a  $\gamma$ -independent potential is assumed [8], while in X(5), related to the transition from vibrational [U(5)] to axially symmetric prolate [SU(3)] nuclei, a potential of the form  $u(\beta) + u(\gamma)$

---

<sup>1</sup>e-mail: ruben.fossion@pd.infn.it

<sup>2</sup>e-mail: bonat@inp.demokritos.gr

<sup>3</sup>e-mail: glalazis@auth.gr

is used. A systematic study of phase transitions in nuclear collective models has been given in [9, 10, 11].

It is of interest to examine if the assumption of a relatively flat potential in the E(5) and X(5) models is justified through the use of a completely different method, as the Relativistic Mean Field (RMF) approach [12] using the NL3 effective force, the parameter set of which has been fixed by fitting ground state properties of spherical nuclei [13]. The calculation of Potential Energy Surfaces (PES) for a series of isotopes in which a critical nucleus appears should result in a relatively flat PES for this particular nucleus.

Furthermore, the question of a prolate to oblate shape phase transition, expected to take place in the Pt region, has been raised recently [14]. RMF theory [12] is a suitable tool for locating the prolate to oblate shape transition in the Pt series of isotopes.

The Relativistic Hartree Bogoliubov model used in the present work is briefly described in Section 2. In this variation of the RMF theory, pairing correlations are treated in a self consistent manner, since in constrained calculations the correct treatment of pairing is essential for a reliable description of the potential landscapes. RMF theory is then used to produce potential energy surfaces for chains of isotopes involving nuclei suggested to be good examples of the E(5) and X(5) critical point symmetries in Sections 3 and 4 respectively, while in Section 5 a study of isotopic chains related to the prolate to oblate shape transition is given. The main conclusions arising from the present results and plans for further work are finally discussed in Section 6.

## 2 The Relativistic Hartree Bogoliubov model

The model describes the nucleus as a system of Dirac nucleons which interact in a relativistic covariant manner through the exchange of virtual mesons. The relativistic extension of the Hartree Fock Bogoliubov theory is described in detail in Refs. [15, 16]. The generalized single-particle Hamiltonian of HFB theory contains two average potentials: the self consistent field  $\hat{\Gamma}$  which encloses all the long range  $ph$  correlations, and the pairing field  $\hat{\Delta}$  which sums up the  $pp$ -correlations. In the Hartree approximation for the self-consistent mean field, the Relativistic Hartree-Bogoliubov equations read

$$\begin{pmatrix} \hat{h}_D - m - \lambda & \hat{\Delta} \\ -\hat{\Delta}^* & -\hat{h}_D + m + \lambda \end{pmatrix} \begin{pmatrix} U_k(\mathbf{r}) \\ V_k(\mathbf{r}) \end{pmatrix} = E_k \begin{pmatrix} U_k(\mathbf{r}) \\ V_k(\mathbf{r}) \end{pmatrix}, \quad (1)$$

where  $m$  is the nucleon mass and  $\hat{h}_D$  is the single-nucleon Dirac Hamiltonian

$$\left\{ -i\boldsymbol{\alpha} \cdot \boldsymbol{\nabla} + \beta(m + g_\sigma \sigma) + g_\omega \omega^0 + g_\rho \tau_3 \rho_3^0 + e \frac{(1 - \tau_3)}{2} A^0 \right\} \psi_i = \varepsilon_i \psi_i, \quad (2)$$

with  $\sigma$ ,  $\omega$ , and  $\rho$  the meson fields,  $A$  the electromagnetic potential and  $g_\sigma$ ,  $g_\omega$ , and  $g_\rho$  the corresponding coupling constants of the mesons to the nucleon.

In Eq. (1) the chemical potential  $\lambda$  has to be determined by the particle number subsidiary condition in order that the expectation value of the particle number operator in the ground state equals the number of nucleons.  $\hat{\Delta}$  is the pairing field. The column vectors denote the quasi-particle spinors and  $E_k$  are the quasi-particle energies. The self-consistent solution of the Dirac-Hartree-Bogoliubov integro-differential eigenvalue equations and Klein-Gordon equations for the meson fields determines the nuclear ground state. In the present variation of the model these equations are solved by expanding the nucleon spinors  $U_k(\mathbf{r})$  and  $V_k(\mathbf{r})$ , and the meson fields, in terms of the eigenfunctions of a deformed axially symmetric oscillator potential. The calculations have been performed using the NL3 Lagrangian parametrization [13], which has been proved very successful in describing various nuclear properties at and away from the line of  $\beta$ -stability. Finally, for the pairing field we employ the pairing part of the Gogny interaction [17]. The basic advantage of this choice is the fact that the Gogny force has a finite range which automatically guarantees a proper cut-off in momentum space.

### 3 The E(5) shape phase transition

The first nucleus to be identified as exhibiting E(5) behaviour was  $^{134}\text{Ba}$  [3], while  $^{102}\text{Pd}$  [18, 19] also seems to provide a very good candidate. Further studies on  $^{134}\text{Ba}$  [20] reinforced this conclusion, while  $^{108}\text{Pd}$  has been suggested [21] to be an E(5) candidate and  $^{100}\text{Pd}$  was found [22] to correspond to a numerical solution using a  $\beta^4$  potential [23, 24] instead of an infinite square well potential in the E(5) framework. A systematic search [5, 25] on available data on energy levels and B(E2) transition rates also singled out  $^{128}\text{Xe}$  as a good candidate.  $^{130}\text{Xe}$  has also been suggested [26] as a possible candidate, in agreement with a recent report [27] on measurements of E1 and M1 strengths of  $^{124-136}\text{Xe}$ , which provide evidence for a shape phase transition around  $A \simeq 130$ .

Potential energy surfaces for  $^{96-114}\text{Pd}$ ,  $^{118-134}\text{Xe}$ , and  $^{118-138}\text{Ba}$  are shown in Figs. 1-3.  $^{100}\text{Pd}$  and  $^{102}\text{Pd}$  show PES which are quite flat. The PES of  $^{108}\text{Pd}$  and  $^{110}\text{Pd}$  are also quite flat. In addition, it is clear that  $^{126-130}\text{Xe}$  do exhibit flat PES, being on the way from vibrational behaviour, seen in  $^{134}\text{Xe}$  ( $R_4 = 2.044$  [28]), to  $\gamma$ -unstable behaviour in the lighter Xe isotopes [29]. Similarly,  $^{132-134}\text{Ba}$  exhibit rather flat PES, being on the way from vibrational behaviour, seen in  $^{136}\text{Ba}$  ( $R_4 = 2.280$  [28]), to  $\gamma$ -unstable behaviour in the lighter Ba isotopes.

In general, we remark that the assumption of a rather flat potential in the E(5) critical point symmetry is supported quite well by the present calculations in the nuclei which have been suggested as good E(5) examples.

## 4 The X(5) shape phase transition

The first nucleus to be identified as exhibiting X(5) behaviour was  $^{152}\text{Sm}$  [4], followed by  $^{150}\text{Nd}$  [30]. Further work on  $^{152}\text{Sm}$  [31, 32, 33, 34] and  $^{150}\text{Nd}$  [32, 33, 35] reinforced this conclusion. The neighbouring N=90 isotones  $^{154}\text{Gd}$  [36, 37] and  $^{156}\text{Dy}$  [37, 38] were also seen to provide good X(5) examples, the latter being of less good quality. A systematic study [6] of available experimental data on energy levels and B(E2) transition rates suggested  $^{126}\text{Ba}$  as a possible good candidate, in addition to the N=90 isotones of Nd, Sm, Gd, and Dy.  $^{122}\text{Ba}$  has also been recently suggested [39] as a possible candidate. In parallel,  $^{148}\text{Nd}$  has been suggested as corresponding to an analytic solution [40] using a  $\beta^2$  potential instead of an infinite square well potential within the X(5) framework.

Potential energy surfaces for  $^{144-156}\text{Nd}$ ,  $^{146-158}\text{Sm}$ ,  $^{148-156}\text{Gd}$ , and  $^{150-158}\text{Dy}$  are shown in Figs. 4-7, while PES for  $^{118-138}\text{Ba}$  have already been exhibited in Fig. 3. We remark that for all of the above mentioned nuclei [ $^{122,126}\text{Ba}$ ,  $^{150}\text{Nd}$ ,  $^{152}\text{Sm}$ ,  $^{154}\text{Gd}$ ,  $^{156}\text{Dy}$ ] the PES is not flat, exhibiting a deeper minimum in the prolate ( $\beta_2 > 0$ ) regime and a shallower minimum in the oblate ( $\beta_2 < 0$ ) region. Relatively flat PES occur for the N=86 nuclei  $^{146}\text{Nd}$ ,  $^{148}\text{Sm}$ ,  $^{150}\text{Gd}$ , and  $^{152}\text{Dy}$  (to a lesser extend).

The present results for  $\beta_2 > 0$  are in good agreement with the PES obtained for  $^{144-158}\text{Sm}$  by Relativistic Mean Field (RMF) theory in Ref. [41], using the NL3 force, as well as the NL1, NLSH and TM1 forces. In Ref. [41] the PES for  $^{152}\text{Sm}$ , as well as for neighbouring nuclei, presents a single minimum in the region  $\beta_2 > 0$ , in agreement with Fig. 5. Furthermore the present results for  $^{146-156}\text{Sm}$  and  $^{154}\text{Gd}$  are in good agreement with Nilsson-Strutinsky-BCS calculations [42].

From the above we conclude that the present results, in agreement with earlier calculations, do not predict flat PES for the N=90 isotones, which are the best experimental manifestations of X(5). However, the existence of a bump in the PES corresponding to good experimental examples of X(5) might be related to the success of the confined  $\beta$ -soft (CBS) rotor model [43, 44], employing an infinite square well potential displaced from zero, as well as to the relevance of Davidson potentials [45, 46] of the form  $\beta^2 + \beta_0^4/\beta^2$  (where  $\beta_0$  is the minimum of the potential) in the description of X(5) properties [47, 48]. It can also be related to the significant five-dimensional centrifugal effect [49], found recently through the use of novel techniques allowing for the exact numerical diagonalization of the Bohr Hamiltonian [50, 51, 52].

## 5 The prolate to oblate transition

The chain of nuclei  $^{180}\text{Hf}$ ,  $^{182,184,186}\text{W}$ ,  $^{188,190,192}\text{Os}$ ,  $^{194,196}\text{Pt}$ , and  $^{198,200}\text{Hg}$  has been suggested [14], on the basis of experimental data, as exhibiting a transition from prolate to oblate shapes at  $^{194}\text{Pt}$ . The PES shown in Fig. 8 clearly show such a transition, since the prolate minimum is lower than the oblate minimum up to  $^{192}\text{Os}$ , while in  $^{194}\text{Pt}$  the opposite picture appears. The PES for  $^{194}\text{Pt}$  and especially for  $^{196}\text{Pt}$  is flat, evolving in  $^{198}\text{Hg}$  and  $^{200}\text{Hg}$  towards a vibrational shape. The quadrupole moments of the nuclei belonging to this chain, shown in Fig. 9, also exhibit the transition from negative values (corresponding to prolate shapes) to positive values (corresponding to oblate shapes). It should be noticed that in Fig. 9 (as well as in similar subsequent figures) the experimental values should be compared to the theoretical results for the total quadrupole moments, while the theoretical results for the separate contributions of the protons and of the neutrons are shown for completeness. It is, however, worth remarking that the experimental values are close to the theoretical contributions of the protons.

It should be noticed, however, that the PES of the  $^{184-202}\text{Pt}$  isotopes, shown in Fig. 10, exhibit a transition from prolate to oblate shapes between  $^{186}\text{Pt}$  (prolate) and  $^{188}\text{Pt}$  (oblate). In  $^{184-192}\text{Pt}$  two minima appear, the prolate minimum being lower than the oblate minimum in  $^{184,186}\text{Pt}$ , with the opposite situation occurring in  $^{188-192}\text{Pt}$ . Beyond  $^{194}\text{Pt}$  the PES becomes flat, evolving towards a vibrational shape, reached at  $^{202}\text{Pt}$ . The quadrupole moments of  $^{184-202}\text{Pt}$ , shown in Fig. 11, also exhibit a transition from prolate to oblate behaviour between  $^{186}\text{Pt}$  and  $^{188}\text{Pt}$ .

The prediction that the nucleus  $^{186}\text{Pt}$  is critical is supported by several pieces of evidence. As seen in Fig. 12, the  $\beta_1$ -bandheads (normalized to the energy of the  $2_1^+$  state) exhibit a minimum at  $^{186}\text{Pt}$ , while the crossover of the (normalized to the energy of the  $2_1^+$  state) bandheads of the  $\beta_1$  and  $\gamma_1$  bands also occurs at the same nucleus. Furthermore, mapping the Pt isotopic chain on the symmetry triangle [53] of the Interacting Boson Model [29] shows [54] that  $^{186}\text{Pt}$  lies very close to the shape phase coexistence region of IBM [55, 56].

A similar transition from prolate to oblate shapes is seen in the  $^{188-200}\text{Os}$  chain, shown in Fig. 13. The prolate minimum is lower than the oblate minimum in  $^{188-192}\text{Os}$ , while the opposite situation occurs in  $^{194,196}\text{Os}$ . In  $^{196}\text{Os}$  the PES is already quite flat, evolving towards a vibrational shape in  $^{200}\text{Os}$ . The quadrupole moments for  $^{188-200}\text{Os}$ , shown in Fig. 14, also suggest a transition from prolate to oblate shapes between  $^{192}\text{Os}$  and  $^{194}\text{Os}$ .

## 6 Discussion

The present calculations of Potential Energy Surfaces (PES) in the Relativistic Mean Field theory using the NL3 force lead to the following main conclusions.

a) The assumption made in the E(5) critical point symmetry that the potential in  $\beta$  can be approximated by an infinite square well potential is justified, since rather flat PES are found for nuclei suggested as good examples of E(5).

b) The PES found for nuclei suggested as good examples of X(5) exhibit a bump, in agreement with earlier calculations [41, 42]. The presence of a bump might be related to the success of the confined  $\beta$ -soft (CBS) rotor model [43, 44], the relevance of Davidson potentials in the description of X(5) properties [47, 48], as well as to the existence of a significant five-dimensional centrifugal effect found recently [49].

c) The PES obtained for the series of Pt isotopes suggest a prolate to oblate shape transition at  $^{186}\text{Pt}$ .

It is certainly of interest to calculate PES as functions of  $\beta_2$  and  $\gamma$ , in order to examine to which extent the above conclusions are influenced by the  $\gamma$  degree of freedom. In particular, one should examine carefully the PES in which two minima appear, since one of the minima could be a saddle point. In addition it is of interest to examine if and to which extent the present results will be changed if methods beyond the mean field approximation (see, for example, Refs. [57, 58, 59]) are employed.

## Acknowledgements

Partial support from the programme Pythagoras II of the Greek MNE & RA under project 80861 (RF,GAL) and from the Greek State Scholarships Foundation (RF) is gratefully acknowledged.

## References

- [1] F. Iachello, Phys. Rev. Lett. **85**, 3580 (2000).
- [2] F. Iachello, Phys. Rev. Lett. **87**, 052502 (2001).
- [3] R. F. Casten and N. V. Zamfir, Phys. Rev. Lett. **85**, 3584 (2000).
- [4] R. F. Casten and N. V. Zamfir, Phys. Rev. Lett. **87**, 052503 (2001).
- [5] R. M. Clark, M. Cromaz, M. A. Deleplanque, M. Descovich, R. M. Diamond, P. Fallon, I. Y. Lee, A. O. Macchiavelli, H. Mahmud, E. Rodriguez-Vieitez, F. S. Stephens, and D. Ward, Phys. Rev. C **69**, 064322 (2004).
- [6] R. M. Clark, M. Cromaz, M. A. Deleplanque, M. Descovich, R. M. Diamond, P. Fallon, R. B. Fierstone, I. Y. Lee, A. O. Macchiavelli, H. Mahmud, E. Rodriguez-Vieitez, F. S. Stephens, and D. Ward, Phys. Rev. C **68**, 037301 (2003).
- [7] A. Bohr, Mat. Fys. Medd. K. Dan. Vidensk. Selsk. **26**, no. 14 (1952).
- [8] L. Wilets and M. Jean, Phys. Rev. **102**, 788 (1956).
- [9] D. J. Rowe, Nucl. Phys. A **745**, 47 (2004).
- [10] P. S. Turner and D. J. Rowe, Nucl. Phys. A **756**, 333 (2005).
- [11] G. Rosensteel and D. J. Rowe, Nucl. Phys. A **759**, 92 (2005).
- [12] D. Vretenar, A. V. Afanasjev, G. A. Lalazissis, and P. Ring, Physics Reports **409**, 101 (2005).
- [13] G. A. Lalazissis, J. König, and P. Ring, Phys. Rev. C **55**, 540 (1997).
- [14] J. Jolie and A. Linnemann, Phys. Rev. C **68**, 031301 (2003).
- [15] H. Kucharek and P. Ring, Z. Phys. A **339**, 23 (1991).
- [16] G. A. Lalazissis, D. Vretenar, and P. Ring, Nucl. Phys. A **650**, 133 (1999).
- [17] J.F. Berger, M. Girod and D. Gogny, Nucl. Phys. A **428**, 32 (1984).
- [18] N. V. Zamfir, M. A. Caprio, R. F. Casten, C. J. Barton, C. W. Beausang, Z. Berant, D. S. Brenner, W. T. Chou, J. R. Cooper, A. A. Hecht, R. Krücken, H. Newman, J. R. Novak, N. Pietralla, A. Wolf, and K. E. Zyromski, Phys. Rev. C **65**, 044325 (2002).

- [19] G. Kalyva, A. Spyrou, M. Axiotis, S. Harissopulos, A. Dewald, A. Fitzler, B. Saha, A. Linnemann, O. Möller, R. Vlastou, D. R. Napoli, N. Marginean, C. Rusu, G. de Angelis, C. Ur, D. Bazzacco, E. Farnea, D. L. Balabanski, and R. Julin, in *Frontiers in Nuclear Structure, Astrophysics and Reactions (Kos 2005)*, edited by R. Julin and S. Harissopulos (2005).
- [20] J. M. Arias, Phys. Rev. C **63**, 034308 (2001).
- [21] D.-L. Zhang and Y.-X. Liu, Phys. Rev. C **65**, 057301 (2002).
- [22] D. Bonatsos, D. Lenis, N. Minkov, P. P. Raychev, and P. A. Terziev, Phys. Rev. C **69**, 044316 (2004).
- [23] J. M. Arias, C. E. Alonso, A. Vitturi, J. E. García-Ramos, J. Dukelsky, and A. Frank, Phys. Rev. C **68**, 041302 (2003).
- [24] J. E. García-Ramos, J. Dukelsky, and J. M. Arias, Phys. Rev. C **72**, 037301 (2005).
- [25] M. W. Kirson, Phys. Rev. C **70**, 049801 (2004).
- [26] D.-L. Zhang and Y.-X. Liu, Chin. Phys. Lett. **20**, 1028 (2003).
- [27] U. Kneissl, in *Key Topics in Nuclear Structure (Paestum 2004)*, edited by A. Covello (World Scientific, Singapore, 2005) p. 399.
- [28] Nuclear Data Sheets, as of June 2005.
- [29] F. Iachello and A. Arima, *The Interacting Boson Model* (Cambridge University Press, Cambridge, 1987).
- [30] R. Krücken, B. Albanna, C. Bialik, R. F. Casten, J. R. Cooper, A. Dewald, N. V. Zamfir, C. J. Barton, C. W. Beausang, M. A. Caprio, A. A. Hecht, T. Klug, J. R. Novak, N. Pietralla, and P. von Brentano, Phys. Rev. Lett. **88**, 232501 (2002).
- [31] N. V. Zamfir, H. G. Börner, N. Pietralla, R. F. Casten, Z. Berant, C. J. Barton, C. W. Beausang, D. S. Brenner, M. A. Caprio, J. R. Cooper, A. A. Hecht, K. Krtička, R. Krücken, P. Mutti, J. R. Novak, and A. Wolf, Phys. Rev. C **65**, 067305 (2002).
- [32] R. M. Clark, M. Cromaz, M. A. Deleplanque, R. M. Diamond, P. Fallon, A. Görgen, I. Y. Lee, A. O. Macchiavelli, F. S. Stephens, and D. Ward, Phys. Rev. C **67**, 041302 (2003).

- [33] R. F. Casten, N. V. Zamfir, and R. Krücken, *Phys. Rev. C* **68**, 059801 (2003).
- [34] R. Bijker, R. F. Casten, N. V. Zamfir, and E. A. McCutchan, *Phys. Rev. C* **68**, 064304 (2003). Erratum: *Phys. Rev. C* **69**, 059901 (2004).
- [35] D.-L. Zhang and H.-Y. Zhao, *Chin. Phys. Lett.* **19**, 779 (2002).
- [36] D. Tonev, A. Dewald, T. Klug, P. Petkov, J. Jolie, A. Fitzler, O. Möller, S. Heinze, P. von Brentano, and R. F. Casten, *Phys. Rev. C* **69**, 034334 (2004).
- [37] A. Dewald, O. Möller, D. Tonev, A. Fitzler, B. Saha, K. Jessen, S. Heinze, A. Linnemann, J. Jolie, K. O. Zell, P. von Brentano, P. Petkov, R. F. Casten, M. Caprio, J. R. Cooper, R. Krücken, V. Zamfir, D. Bazzacco, S. Lunardi, C. Rossi Alvarez, F. Brandolini, C. Ur, G. de Angelis, D. R. Napoli, E. Farnea, N. Marginean, T. Martinez, and M. Axiotis, *Eur. Phys. J A* **20**, 173 (2004).
- [38] M. A. Caprio, N. V. Zamfir, R. F. Casten, C. J. Barton, C. W. Beausang, J. R. Cooper, A. A. Hecht, R. Krücken, H. Newman, J. R. Novak, N. Pietralla, A. Wolf, and K. E. Zyromski, *Phys. Rev. C* **66**, 054310 (2002).
- [39] C. Fransen, N. Pietralla, A. Linnemann, V. Werner, and R. Bijker, *Phys. Rev. C* **69**, 014313 (2004).
- [40] D. Bonatsos, D. Lenis, N. Minkov, P. P. Raychev, and P. A. Terziev, *Phys. Rev. C* **69**, 014302 (2004).
- [41] J. Meng, W. Zhang, S. G. Zhou, H. Toki, and L. S. Geng, *Eur. Phys. J. A* **25**, 23 (2005).
- [42] J.-Y. Zhang, M. A. Caprio, N. V. Zamfir, and R. F. Casten, *Phys. Rev. C* **60**, 061304 (1999).
- [43] N. Pietralla and O. M. Gorbachenko, *Phys. Rev. C* **70**, 011304 (2004).
- [44] K. Dusling and N. Pietralla, *Phys. Rev. C* **72**, 011303 (2005).
- [45] P. M. Davidson, *Proc. R. Soc.* **135**, 459 (1932).
- [46] D. J. Rowe and C. Bahri, *J. Phys. A* **31**, 4947 (1998).
- [47] D. Bonatsos, D. Lenis, N. Minkov, D. Petrellis, P. P. Raychev, and P. A. Terziev, *Phys. Lett. B* **584**, 40 (2004).

- [48] D. Bonatsos, D. Lenis, N. Minkov, D. Petrellis, P. P. Raychev, and P. A. Terziev, *Phys. Rev. C* **70**, 024305 (2004).
- [49] M. A. Caprio, *Phys. Rev. C* **72**, 054323 (2005).
- [50] D. J. Rowe, *Nucl. Phys. A* **735**, 372 (2004).
- [51] D. J. Rowe, P. S. Turner, and J. Repka, *J. Math. Phys.* **45**, 2761 (2004).
- [52] D. J. Rowe and P. S. Turner, *Nucl. Phys. A* **753**, 94 (2005).
- [53] R. F. Casten, *Nuclear Structure from a Simple Perspective* (Oxford University Press, Oxford, 1990).
- [54] E. A. McCutchan, R. F. Casten, and N. V. Zamfir, *Phys. Rev. C* **71**, 061301 (2005).
- [55] F. Iachello, N. V. Zamfir, and R. F. Casten, *Phys. Rev. Lett.* **81**, 1191 (1998).
- [56] E. A. McCutchan, N. V. Zamfir, and R. F. Casten, *Phys. Rev. C* **69**, 064306 (2004).
- [57] M. Bender, P. Bonche, T. Duguet, and P.-H. Heenen, *Phys. Rev. C* **69**, 064303 (2004).
- [58] R. R. Rodriguez-Guzman, J. L. Egido, and L. M. Robledo, *Phys. Rev. C* **69**, 054319 (2004).
- [59] J. L. Egido and L. M. Robledo, in *Lecture Notes in Physics*, edited by G. Lalazissis, P. Ring, and D. Vretenar (Springer-Verlag, Heidelberg, 2004), Vol. **641**, p. 269.

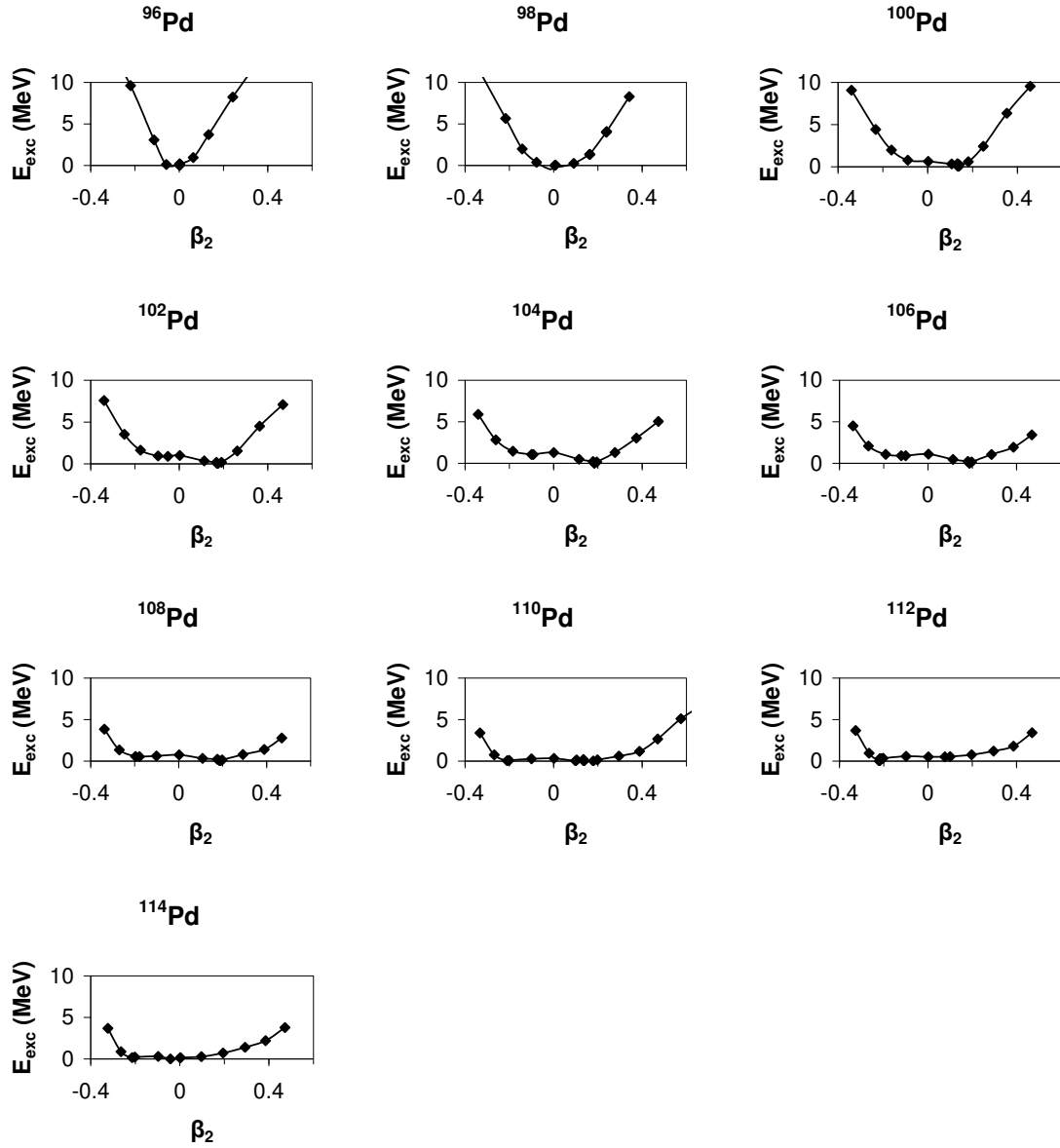


Figure 1: (Color online) Potential energy surfaces (PES) for  $^{96-114}\text{Pd}$ , calculated using the Relativistic Hartree Bogoliubov theory with the NL3 force.

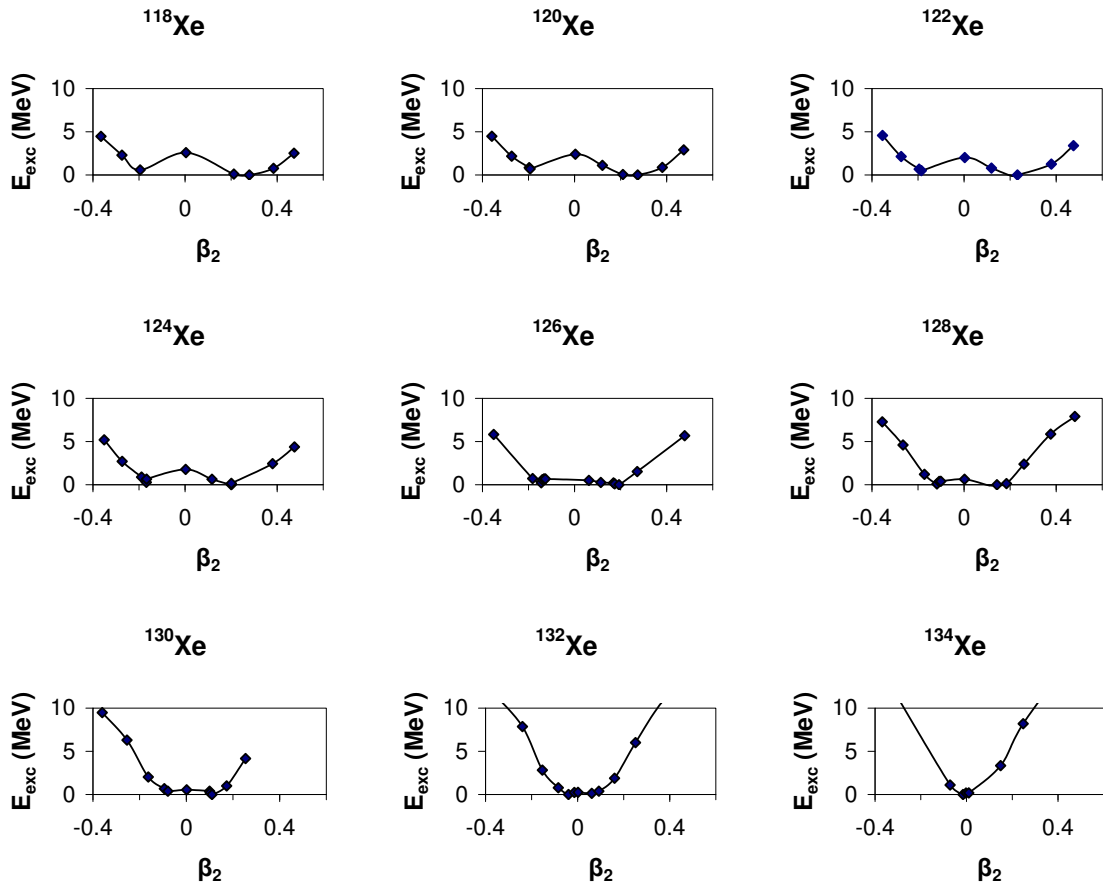


Figure 2: (Color online) Same as Fig. 1, but for  $^{118-134}\text{Xe}$ .

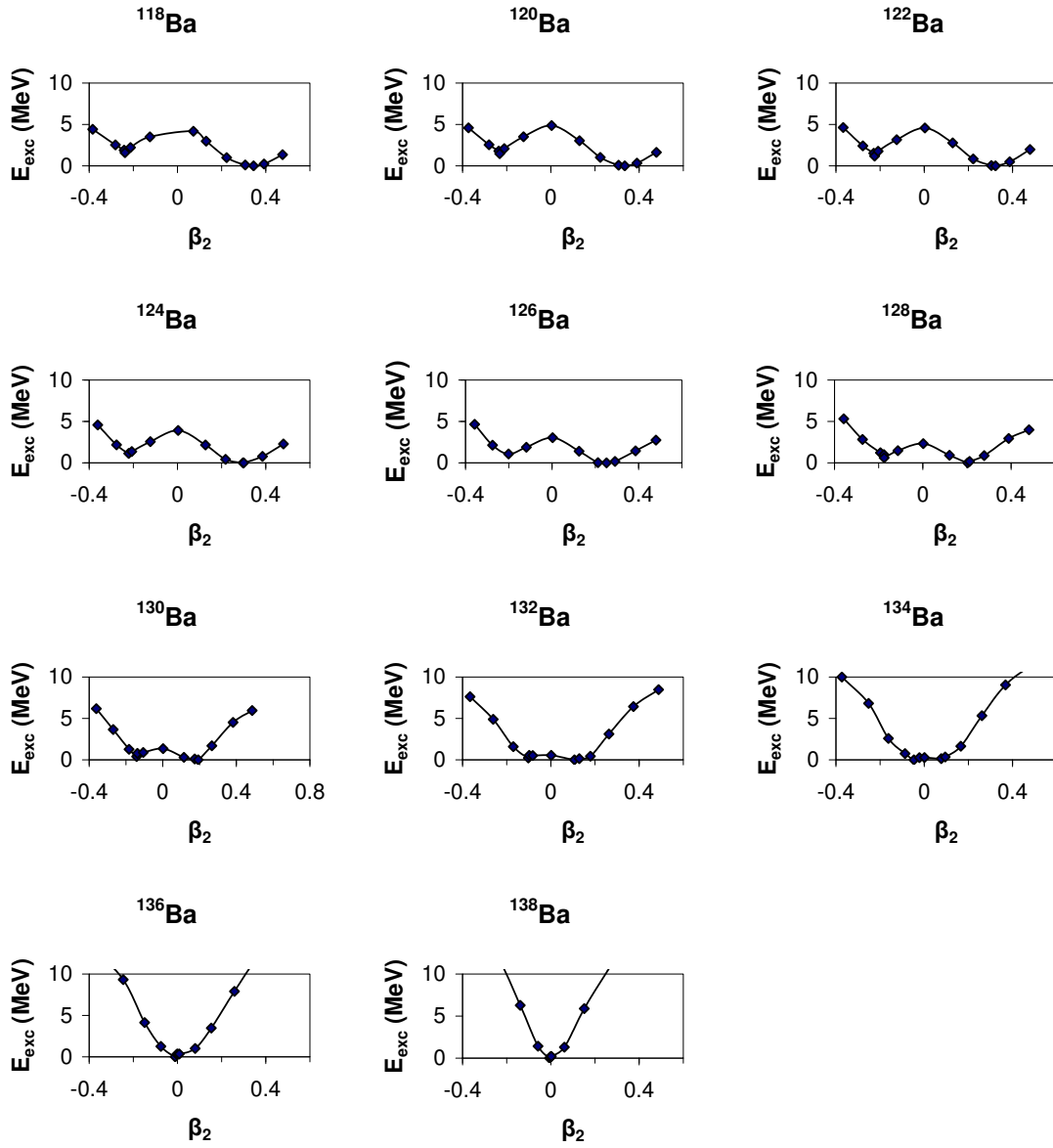


Figure 3: (Color online) Same as Fig. 1, but for  $^{118-138}\text{Ba}$ .

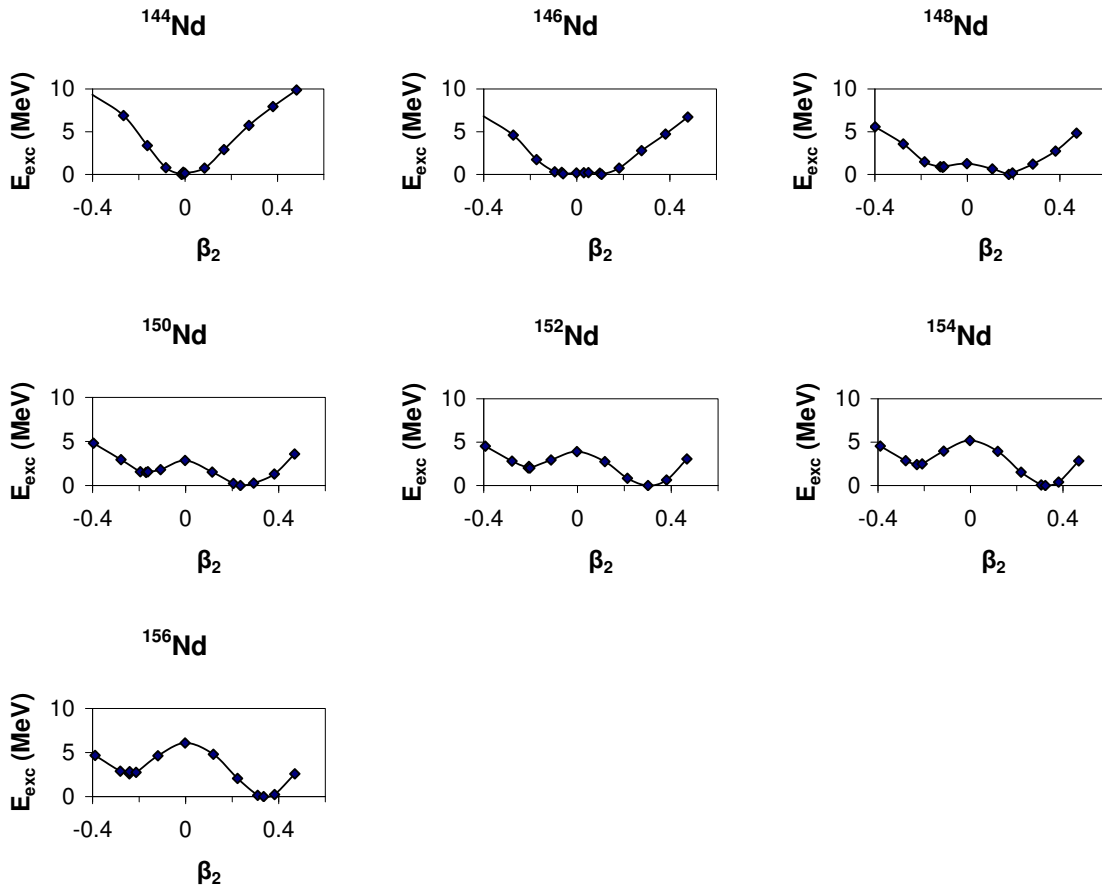


Figure 4: (Color online) Same as Fig. 1, but for  $^{144-156}\text{Nd}$ .

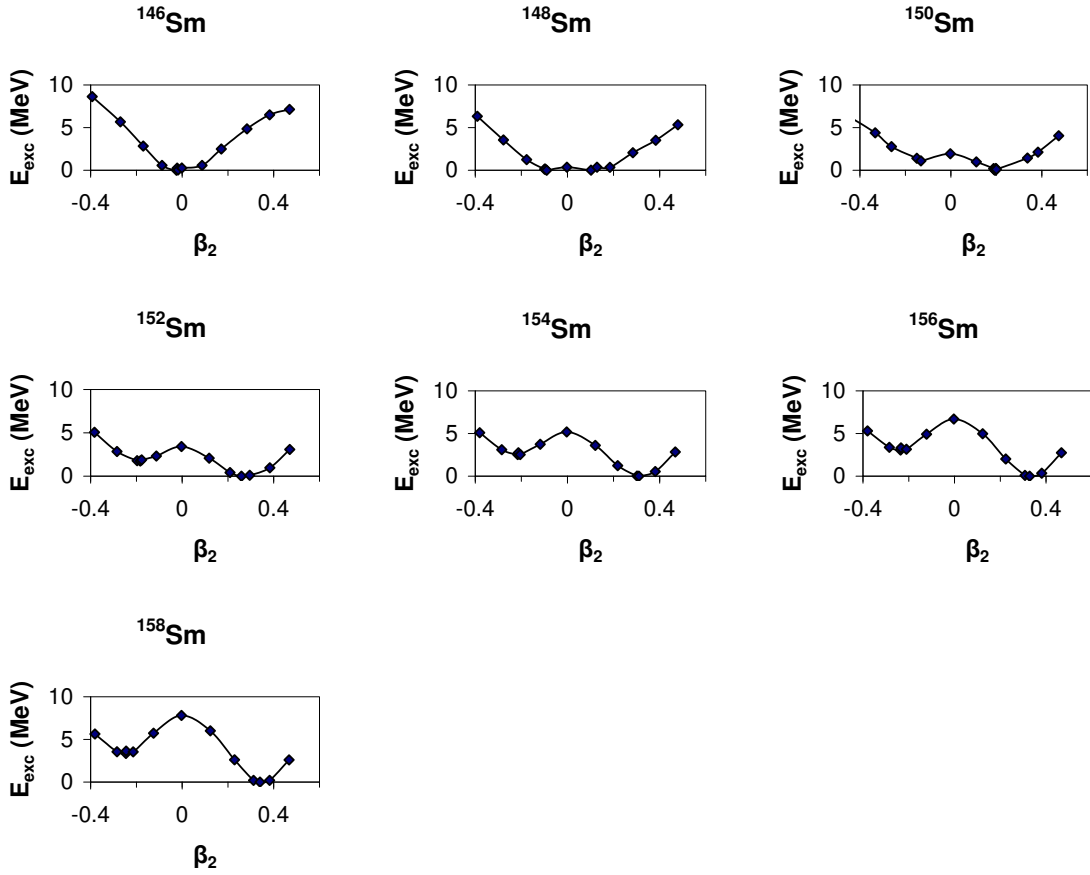


Figure 5: (Color online) Same as Fig. 1, but for  $^{146-158}\text{Sm}$ .

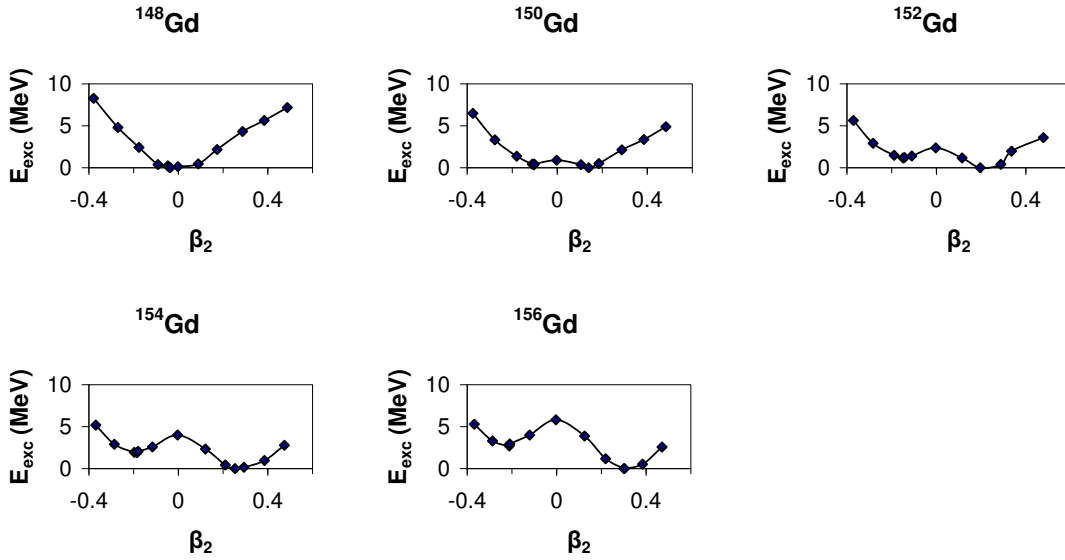


Figure 6: (Color online) Same as Fig. 1, but for  $^{148-156}\text{Gd}$ .

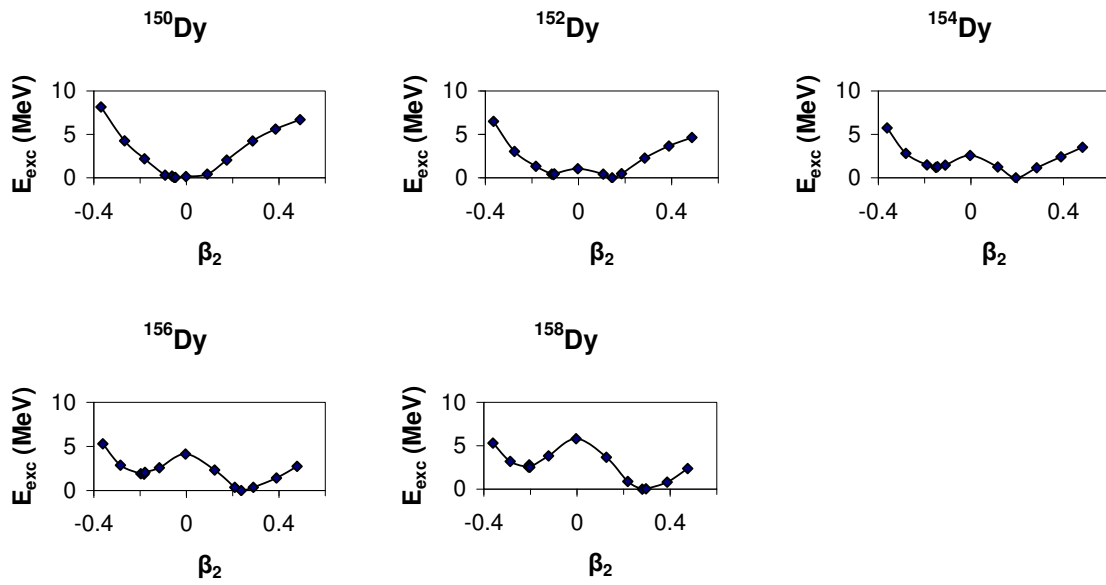


Figure 7: (Color online) Same as Fig. 1, but for  $^{150-158}\text{Dy}$ .

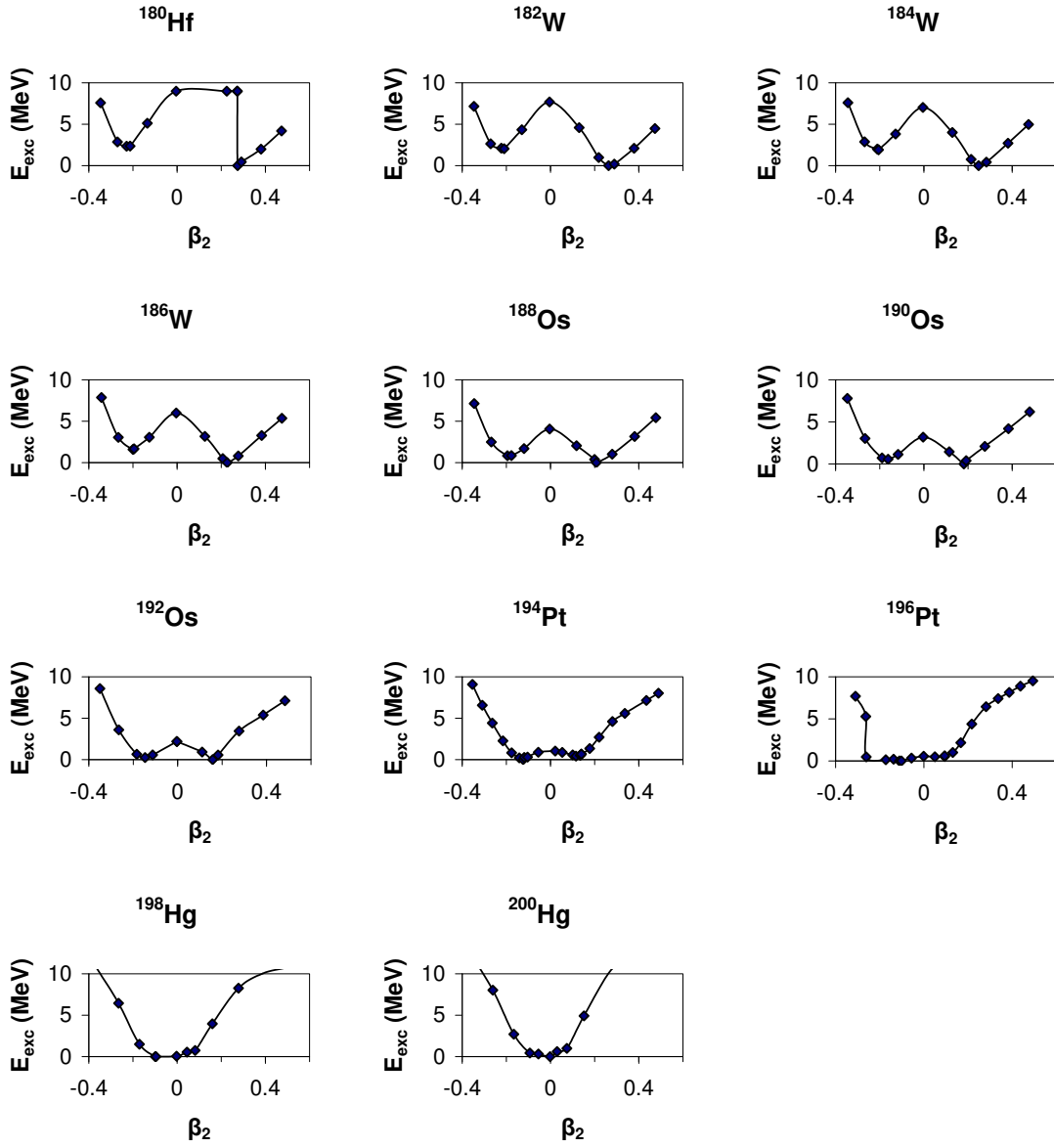


Figure 8: (Color online) Same as Fig. 1, but for  $^{180}\text{Hf}$ ,  $^{182,184,186}\text{W}$ ,  $^{188,190,192}\text{Os}$ ,  $^{194,196}\text{Pt}$ ,  $^{198,200}\text{Hg}$ .

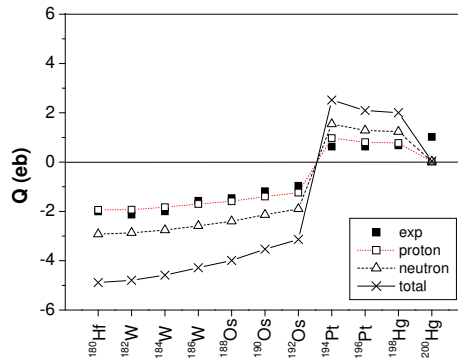


Figure 9: Quadrupole moments for the chain of nuclei of Fig. 8, calculated using the Relativistic Hartree Bogoliubov theory with the NL3 force. Experimental data are taken from Ref. [28].

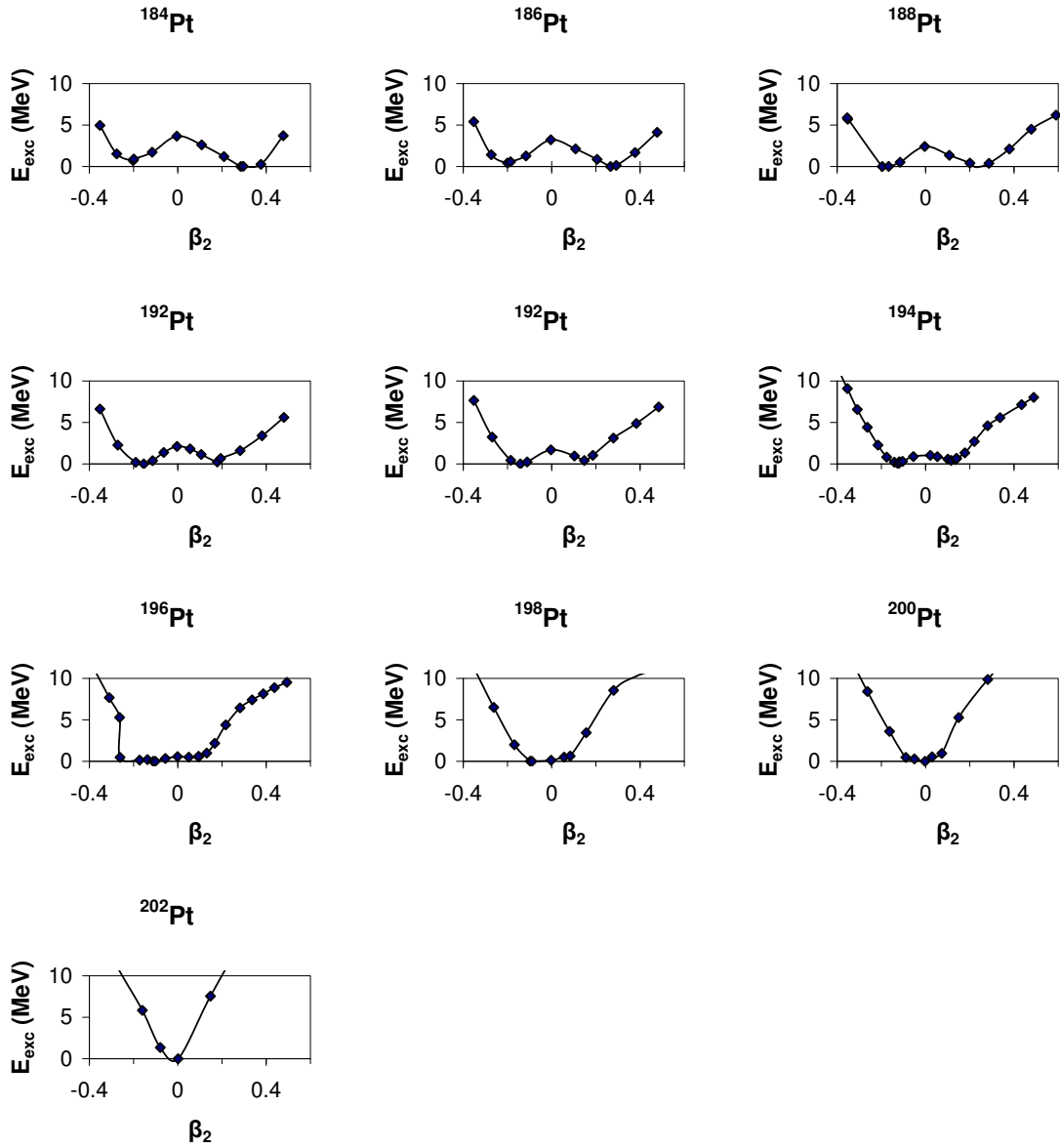


Figure 10: (Color online) Same as Fig. 1, but for  $^{184-202}\text{Pt}$ .

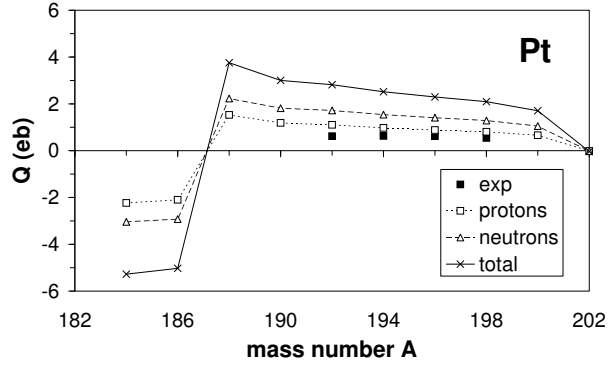


Figure 11: Same as Fig. 9, but for  $^{184-202}\text{Pt}$ . Experimental data are taken from Ref. [28].

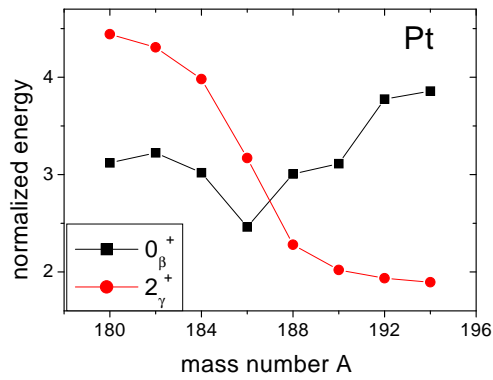


Figure 12: (Color online) Experimental energies of bandheads of the  $\beta_1$  and  $\gamma_1$  bands, normalized to the energy of the  $2^+_1$  state of the ground state band, for several Pt isotopes. Experimental data are taken from Ref. [28].

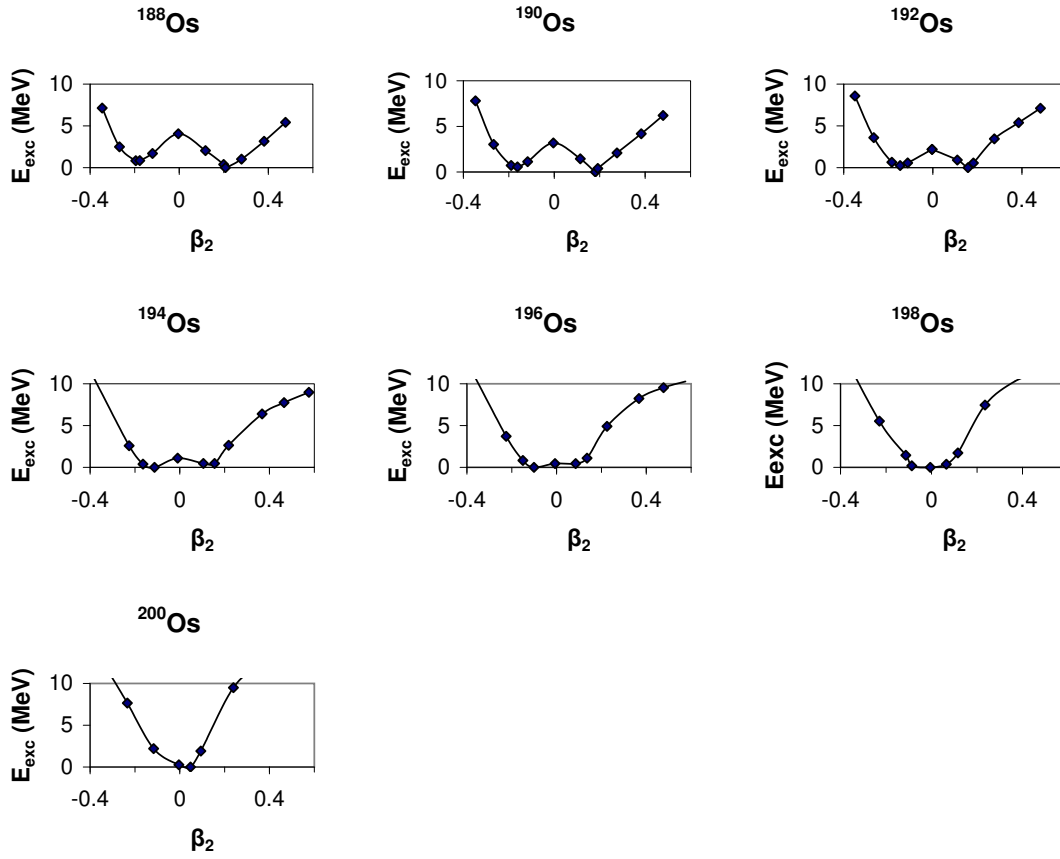


Figure 13: (Color online) Same as Fig. 1, but for  $^{188-200}\text{Os}$ .

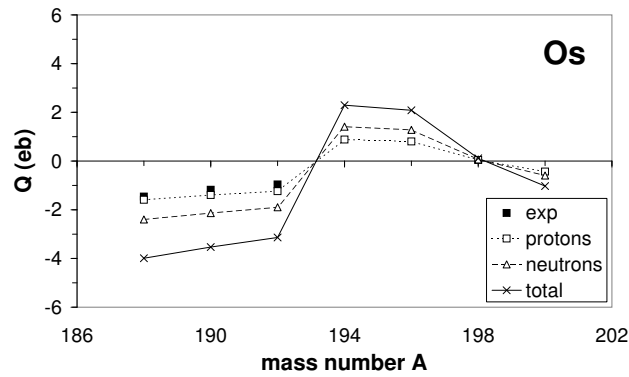


Figure 14: Same as Fig. 9, but for  $^{188-200}\text{Os}$ . Experimental data are taken from Ref. [28].